Coastal Coccolithophores (Guest Ed. R.W. Jordan)
J. Nannoplankton Res., Special Issue, **4**, 2019, pp. 39–54
ISSN 1210-8049 Printed by The Sheridan Press, USA

Distribution of NE Gulf of Mexico nannoplankton assemblages following the Macondo Well blowout: August–November 2011–2013

Jarrett Cruz*, Sherwood W. Wise, Jr, William Parker
Department of Earth, Ocean & Atmospheric Sciences, Florida State University, Tallahassee, FL 32304, USA; *jwc09e@my.fsu.edu

Jeremy R. Young
Department of Earth Sciences, University College London, Gower Street, London, WC1E 6BT, UK

Manuscript received 29th March, 2016; revised manuscript accepted 14th November, 2016

Abstract The biodiversity and biomass of coccolithophore species observed in the NE Gulf of Mexico during August through November of 2011 to 2013 were quite dynamic. Following the Macondo Well blowout in 2010, analyses were carried out on samples taken during the subsequent three years. The photic zone was sampled at 28 sites, along four transects across the continental shelf and slope, in order to observe ecological patterns in the calcareous nannoplankton assemblages. The number of observed species increased from station to station, moving from shallow continental shelf waters into deep water. This was related to a two-layered water configuration, observed during August to November. In moving into the deeper waters, the salinity, temperature and amount of light penetration began to change, which was useful for tracing the thermocline and distinguishing the two layers. Once the depth exceeded 75m, a new assemblage of deeper photic-zone dwellers could be observed. Therefore, two separate nannoplankton assemblages were distinguished, an upper one from the mixed layer, from the surface to 75m depth, and a lower one below the thermocline, from 75m to the lower limits of the photic zone, which for the Gulf of Mexico is 200m. A comparison of site biodiversity and biomass across the stations during the study period also showed an increase in both cell density and number of species observed for each successive year sampled. The lowest cells/L and species diversity were observed in 2011, with increasing numbers in 2012, and the highest recorded in 2013.

Keywords Coccolithophore ecology, Macondo Well, Gulf of Mexico, biodiversity, biomass

1. Introduction

In this study, coccolithophore assemblages were identified that resided in the 200m-deep photic zone in the Gulf of Mexico during August to November from 2011 to 2013. We recorded cell biodiversity and cell density, while tracing the spatial and temporal distribution of observed coccolithophore species, to produce a census for the post-Macondo oilwell blowout interval. The only available pre-blowout quantitative study for comparison was an unpublished dissertation by Vita Pariente (1997). In our study, we aimed to set a baseline for identifying species diversity and abundance, observed vertically and horizontally, in both the genus/species biodiversity and cell density of coccolithophores, from the beginning of our sampling in 2011 to the end in 2013.

2. Study sites, sampling and preparation

Of the three sampling transects, A (Apalachicola), P (Pensacola) and C (Chattahoochee) encompassed nine stations each (Fig. 1, Table 1). At each station, a profile was obtained from within the photic zone, from the surface to a bottom depth of 200m, which is its lower limit in the Gulf of Mexico. The CTD rosette (to measure conductivity, temperature and depth) was lowered to the desired depth, then, as it ascended, attached Niskin bottles were manually triggered, capping the bottles and trapping the water samples. Four fall sampling cruises collected a total of 283 water samples from 29 September through 10 October in 2011, 24 October through 26 October in 2011, 13 October through 15 October in 2012, and 14 September through 16 September in 2013 (Appendix 1).

Once the CTD was back on deck, the water samples were transferred into 1- to 5-L bottles and transported to the shipboard dry lab. The water was filtered aboard ship using a vacuum pump through 44mm-diameter, 0.6μm-pore circular cellulose filters (Bown & Young, 1998). The filters were placed into Petri dishes and oven dried for 4–6 hours at a low temperature to remove excess moisture. After drying, the Petri dishes were placed into sealed bags, and transported to the Florida State University nannofossil laboratory.

Back onshore, in a sterile lab, portions of the filters were mounted onto aluminium stubs using double-sided carbon tape. A corner of the carbon tape was folded over a small portion of the filter membrane to diffuse any charging that might build up while being observed in the scan-

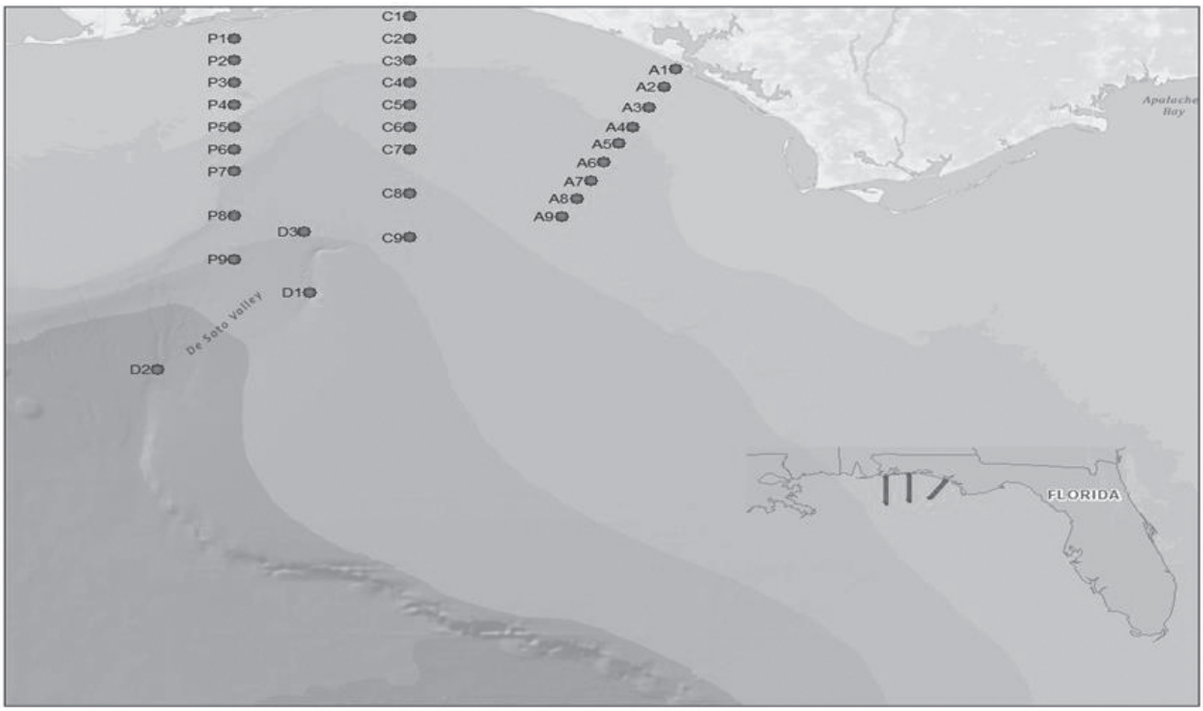

Figure 1: Map of general study area (inset) and sampled sites along transects

Station	Coordinates (Lat +°N↓↑, Lon +°E↓↑)	Station	Coordinates (Lat +°N↓↑, Lon +°E↓↑)	Station	Coordinates (Lat +°N↓↑, Lon +°E↓↑)
A1	30.1333, -85.775	C1	30.1333, -85.775	P1	30.25, -87.25
A2	30.0666, -85.8166	C2	30.25, -86.6666	P2	30.1666, -87.25
A3	29.9916, -85.8666	C3	30.1666, -86.6666	P3	30.0833, -87.25
A4	29.9166, -85.9208	C4	30.0833, -86.6666	P4	30, -87.25
A5	29.8541, -85.9666	C5	30, -86.6666	P5	29.9166, -87.25
A6	29.7833, -86.0166	C6	29.9166, -86.6666	P6	29.8333, -87.25
A7	29.7125, -86.0583	C7	29.8333, -86.6666	P7	29.75, -87.25
A8	29.6458, -86.1083	C8	29.6666, -86.6666	P8	29.5833, -87.25
A9	29.5791, -86.1583	C9	29.5, -86.6666	P9	29.4166, -87.25

Table 1: GPS locations of sites along Transects A, C and P

ning electron microscope (SEM, JXA-840A). The samples were then sputter-coated with gold-palladium under vacuum and argon gas regulation. The prepared stubs were coated to a desired thickness of 10–15nm.

3. Cell counting and identification

Quantitative cell counts of species were recorded from 210 SEM frames, observed at 2500x magnification, using a working distance of 15mm and an accelerating voltage of 30kV, for each of the 283 samples. This method allowed estimations of the filter area examined (Bown & Young, 1998); each frame represented one field of view, covering 0.0005483mm^2 of the filter paper, so cells from a total of 0.115143mm^2 of the filter membrane were counted for each sample. Using these estimations, cells/L were calculated by taking the number of cells observed in a sample (a) and dividing that number by the area of the filter examined (b). This measurement was calculated by using the area of a single field of view at 2500x magnification. This was then divided by the volume of water filtered, in litres (c): (# of cells (a)/area of filter (b))/# of litres filtered (c) = semiquantitative number of cells/L. The cell density data are shown in Figures 2–5.

Coccolithophore species were identified using the systematic definitions primarily from Siesser & Winter (1994) and Young et al. (2003). Another valuable aid for double-

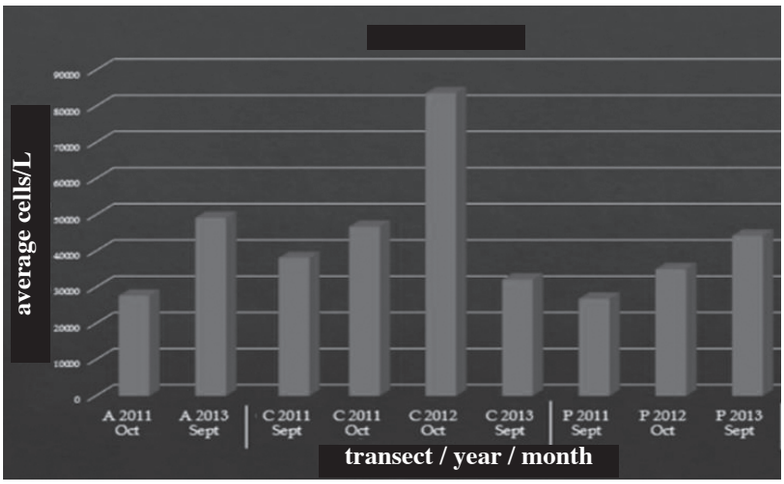

Figure 2: Average cells/L for the sampled intervals

checking the identification of the species was *Nannotax3*, an integrated website for the identification of fossil and living nannoplankton. The taxonomic biodiversity data are shown in Figures 6–9. Species were photographed using software integrated with the SEMs available at the Florida Geological Survey and the Florida State University Physics Department. Images of all of the taxa are illustrated, in alphabetical order, in Plates 1–7, and a list of all taxa is included in Appendix 2.

4. Results

Comparisons of species diversity, relative abundances and changes in species assemblages moving down the water-column were used to identify niche partitioning. The overall pattern observed in the samples was a two-layered system, separating the mixed upper waters from the deep photic waters within the photic zone. The upper 75m of the photic zone and lower 125m (75–200m) revealed different species assemblages. This is similar to the coccolithophore vertical-stratification descriptions given by Brand (1994). In our study, the upper-layer specimens tended to decline in abundance at around 40–75m depth, where deeper-water species began to appear and increase in abundance, until they became dominant in the assemblages below 75m.

This separation in assemblages also correlated with the physical water properties observed in the CTD data. The changeover from upper to lower photic-zone species was traced by an increasing salinity concentration, from 34 to 36 psu at 40 to 75m depth. It was also traced by a decreasing temperature, from 27 to 24°C, marking the thermocline. At the thermocline, the upper photic-zone species became less abundant and began to disappear as the lower photic-zone species appeared and increased in abundance. *Emiliania huxleyi* (Pl. 3, fig. 5), *Gephyrocapsa oceanica* (Pl. 4, fig. 2) and *Umbellosphaera tenuis* (Pl. 7, fig. 3) were observed at most stations, throughout the entire profiles. *Emiliania huxleyi* occurred in high abundances at nearly every station sampled; however, the presence of *U. tenuis* and *G. oceanica* was more variable. At many of the shallower stations, *U. tenuis* and *G. oceanica* were common in the upper photic layer (25–50m maximum depth). Likewise, at many of the deeper stations, they were observed in the upper mixed waters, as well as extending down to the base of the photic zone, like *E. huxleyi*. In the upper mixed waters (1–75m depth), we also saw high abundances of *Calciopappus rigidus* (Pl. 2, fig. 1), *Gephyrocapsa ericsonii* (Pl. 4, fig. 1), *Michaelsarsia adriaticus* (Pl. 5, fig. 5), *Ophiaster formosus* (Pl. 6, fig. 2) and *Umbellosphaera irregularis* (Pl. 7, fig. 2).

In the lower photic zone, we observed different assemblages of species. The major contributor to this layer was *Florisphaera profunda* (Pl. 3, fig. 6), normally found below the thermocline, after a drop in temperature and increase in salinity (Brand, 1994). Other common deep-dwelling species found alongside *F. profunda* were *Algirosphaera robusta* (Pl. 1, fig. 2), *Calcidiscus leptoporus* (Pl. 1, fig. 6), *Gladiolithus flabellatus* (Pl. 4, fig. 3) and *Umbilicosphaera foliosa* (Pl. 7, fig. 5). The rest of the species in the species list (Appendix 2) occurred sporadically throughout the stations.

5. Cell density and biodiversity

During the study interval, the total combined average cell density (cells/L) was calculated for each transect (Fig. 2). This overall average showed an increasing cell density on a year-to-year basis. Many factors control the density of organisms in a given system. Notable increases in temperature and salinity were also observed from 2011 to 2013.

For Transect A (Fig. 3), the average cell density was 28,000 cells/L in October 2011. When sampled again in September 2013, the average cell density showed an increase, to 49,000 cells/L. For transect C (Fig. 4), the av-

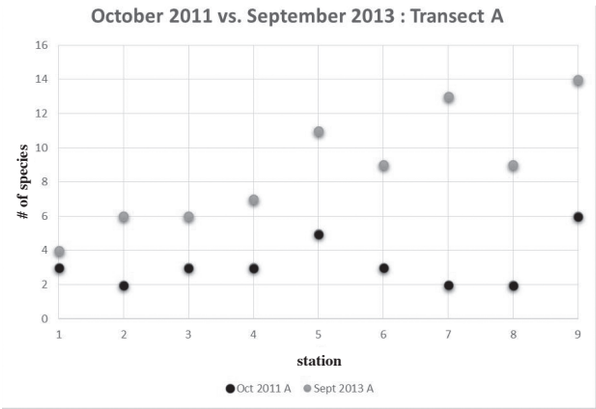

Figure 3: Average cell density of Transect A, October 2011 vs. September 2013

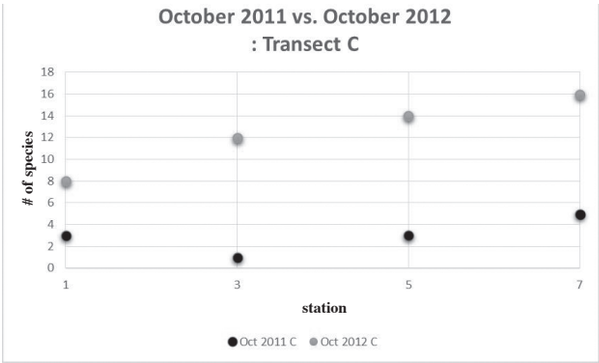

Figure 4: Average cell density of Transect C, October 2011 vs. October 2012

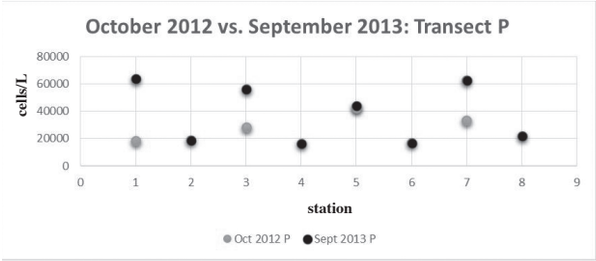

Figure 5: Average cell density of Transect P, October 2012 vs. September 2013

erage cell density was 38,000 cells/L in September 2011 and 47,000 cells/L in October 2011, which is a significant increase within one month. When Transect C was sampled again, in October 2012, it showed a major increase in cell density, with 84,000 cells/L calculated (Fig. 4). Transect P showed a similar pattern, with 27,000 cells/L in September 2011, increasing to 35,073 cells/L in October 2012, with yet another increase in September 2013, to 44,303 cells/L (Fig. 5). (Another transect, D, the farthest offshore, was only sampled in October 2012, and had an average of 65,657 cells/L.)

To get an idea of the biodiversity, the number of different species at each station were recorded for 2011, and then these numbers were compared with those for each successive year that samples were obtained. The overall trend was an increase in biodiversity on a year-to-year basis. The range of increase was one to 11 species; three stations increased by one species, one increased by two, four increased by four, one increased by five, two increased by six, one increased by seven, one by eight, one by nine and four by 11. Only one station (C9) remained constant, with no change in diversity from 2011 to 2013 (Figs 6–9). This increase in biodiversity was associated with an increase in cell density, therefore may be a product of the sampling.

6. Discussion

Common among most of the sampled stations were the prevalent species found throughout the entire sampling interval, from 2011 to 2013. These taxa are thought to have a high tolerance for environmental shifts, and can survive in high stress environments. These species include *A. robusta*, *C. leptoporus*, *E. huxleyi*, *F. profunda*, *G. ericsonii*, *G. oceanica*, *U. irregularis* and *U. tenuis*. These were the most common species found throughout the project.

In 2012 and 2013, the variety of taxa increased, and there was a greater abundance of species that had been observed as only rare in the 2011 samples. These species included *Alveosphaera bimurata*, *C. rigidus*, *Calciosolenia murrayi*, *Michaelsarsia* spp., *Ophiaster formosus*, *Pappomonas* sp. and *Papposphaera* sp. The appearance of these species in the later years could be linked to the pattern of increasing temperature and salinity observed, averaging at around 75m depth, but could also be due to increasing cell density.

There were seven cases where the number of observed species did not increase over the three-year sampling interval. Three of the stations were along Transect C (C5, C6 and C7). The other four were along Transect P (P3, P5, P6 and P8). Nothing obvious, in terms of sampling method or time of day, differed markedly between these and the other samples, so the reason for the decrease in biodiversity is unclear. It could be the result of many different factors, from human error to warm-core eddy interaction. Further investigation into specific atmospheric and oceanic parameters, using eddy modelling programs, as well as the time of day and the conditions in which the samples were recovered, could shed light on the mechanisms that controlled these outliers, and provide a framework for comparison.

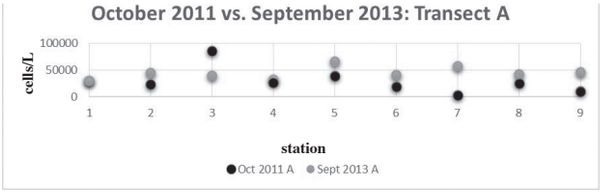

Figure 6: Average biodiversity of Transect A, October 2011 vs. September 2013

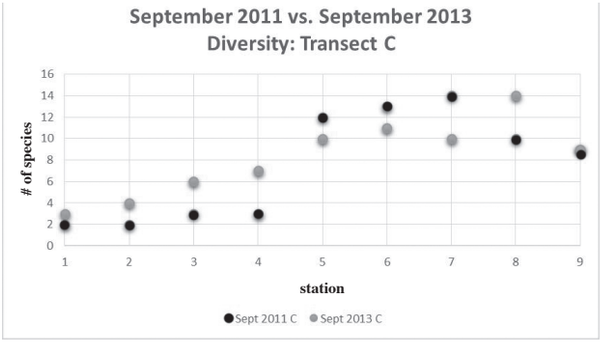

Figure 7: Average biodiversity of Transect C, September 2011 vs. September 2013

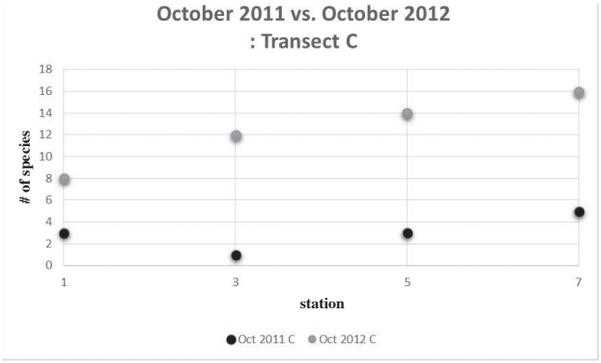

Figure 8: Average biodiversity of Transect C, October 2011 vs. October 2012

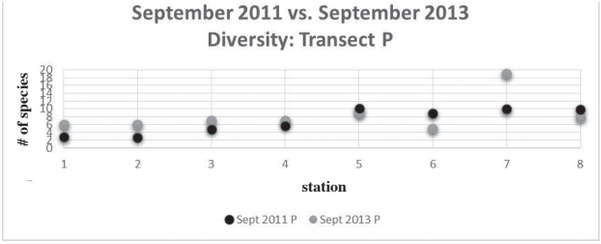

Figure 9: Average biodiversity of Transect P, September 2011 vs. September 2013

The data showed an overall increase in cell density and biodiversity, moving from the nearshore into deeper waters along the transects. This increase in biodiversity at sites moving progressively into deeper waters was due to the two-layered system, defined as an upper mixed layer and a deeper, lower photic-zone layer. This two-layered system allowed for the change from upper (surface to 75m) to lower (75 to 200m) photic-zone assemblages. This significant assemblage change was observed at all sites where the thermocline was penetrated, respresented by a temperature decrease and salinity increase with depth.

The data also presented an increasing trend in biodiversity and cell density with time. The average cell density increased from around 30,000 cells/L in 2011 to 50,000 cells/L in 2013. There was also a gradual increase in the number of species observed in 23 of the 30 stations sampled, from 2011 to 2013. Exactly which ecological parameters controlled this gradual increase is unclear, but an increase in temperature and salinity was also observed from 2011 to 2013. With rare species observed in 2011 becoming more prevalent in 2012 and 2013, along with species not as tolerant to shifts in temperature and salinity that were observed in 2012 and 2013 being absent in 2011, it could be concluded that the system was stabilising from the effects of the 2010 oil spill. The increasing diversity could also be due to the increasing cell density observed through time.

7. Conclusions

Our observations of increasing diversity during a short (three-year) sampling period suggest that not enough data was collected. This increase in diversity could simply correlate to the increasing cells/L observed through time. Rarefaction testing showed little to no change in diversity through time, due to the lower cell counts in the earlier years. This implies that the higher the cell density the more likely rare species would be observed, therefore the increasing diversity could be a product of the sampling.

As observed at Station P7, from October 2012 to September 2013, there was an increase from 33,000 to 63,000 cells/L and a diversity increase from 10 to 19 taxa, including the first observation of *Navilithus altivelum* in the Gulf of Mexico (Cruz et al., 2014). These observations indicate how dynamic the ecological parameters of the Gulf of Mexico are, as well as how imperative additional successive sampling is to better understand the ecology of these coccolithophorids. The cell density increased each successive year; therefore, it might be projected that future sampling would show yet another increase.

Not much is known about the tolerances of most nannoplankton species, or how they react to events that impact their enviroment, such as an oil well blowout, the occurrence of extensive freshwater lenses or shifts in warm-water circulation patterns. The time interval for this

Plate 1

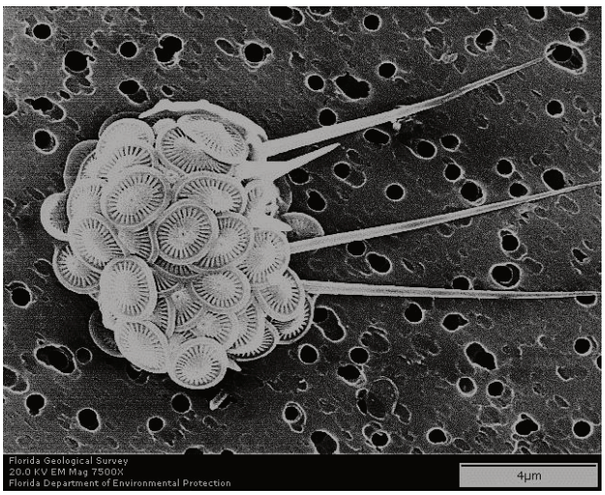

Acanthoica quattrospina

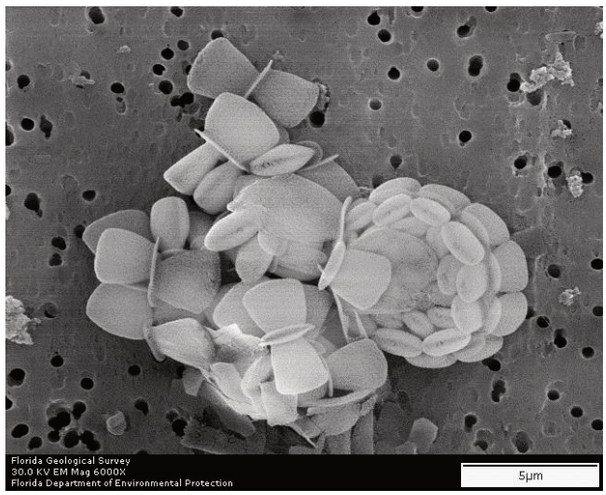

Algirosphaera robusta

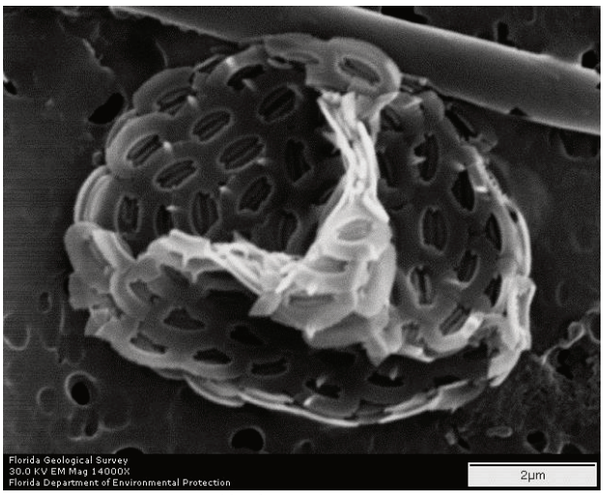

Alisphaera pinnigera

Alveosphaera bimurata

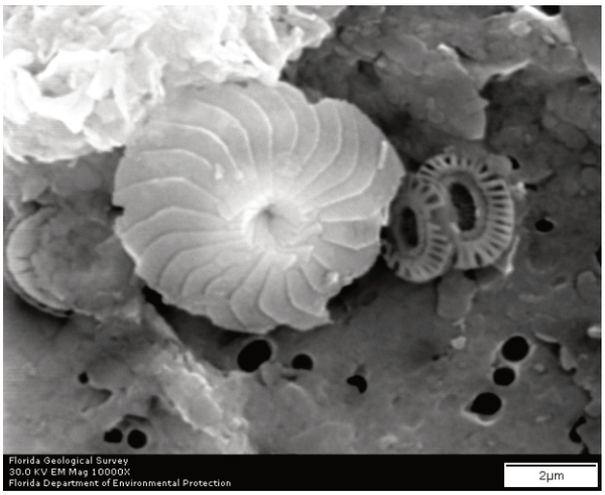

Calcidiscus leptoporus coccolith

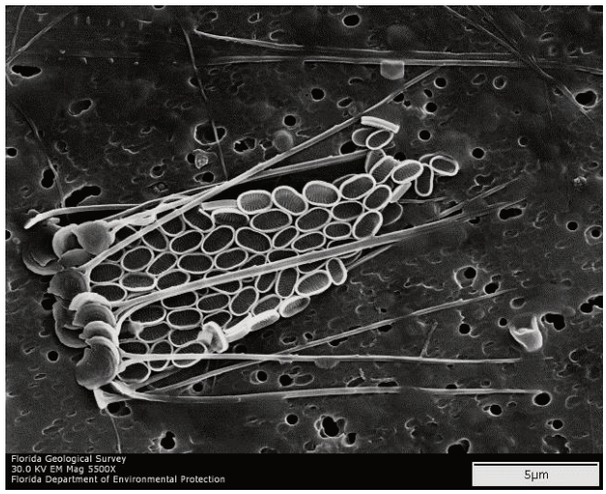

Calciopappus rigidus

Plate 2

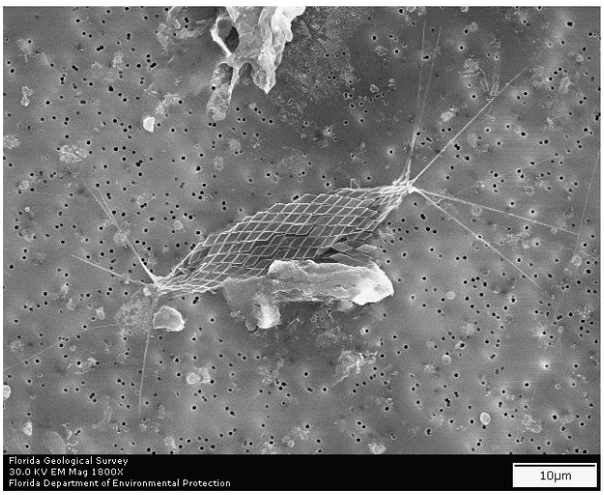

Calciosolenia murrayi

Calicasphaera diconstricta

Calyptrolithina divergens

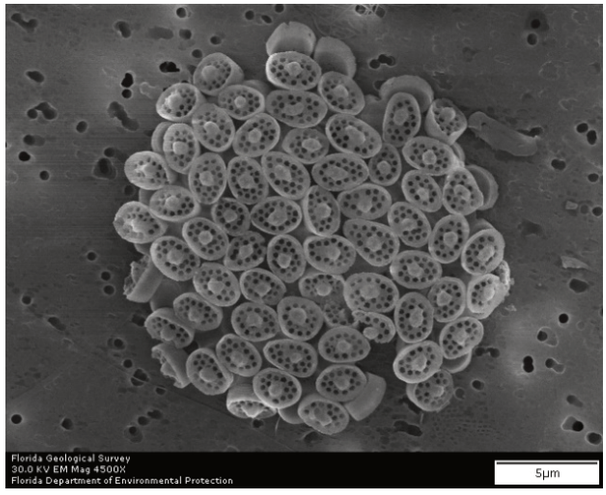

Calyptrolithina multipora

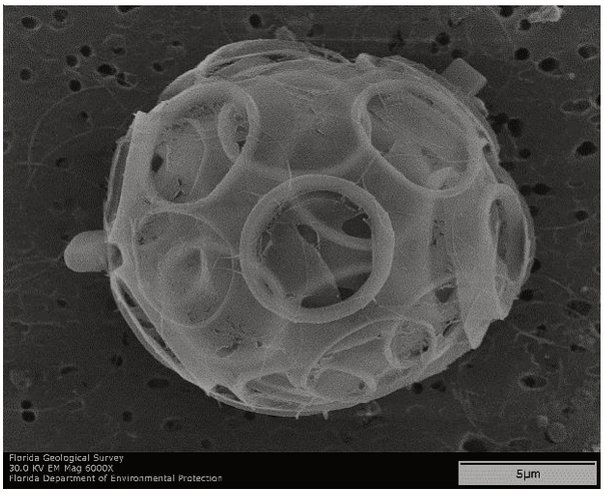

Ceratolithus cristatus HET *coccolithomorpha* type

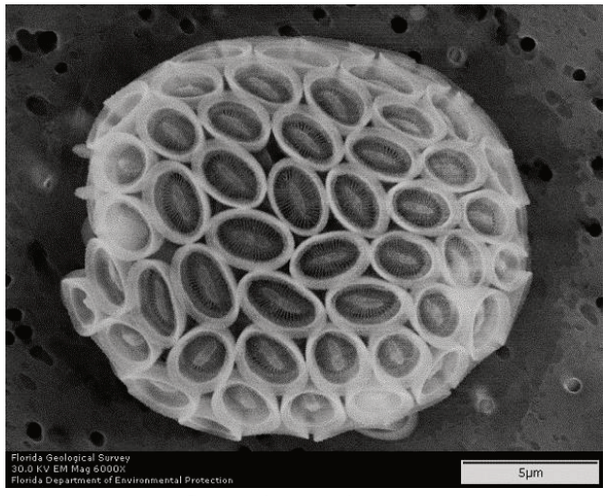

Coronosphaera mediterranea

Plate 3

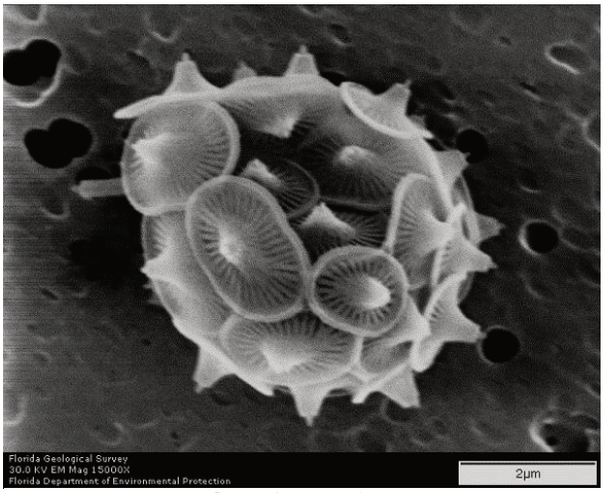

Cyrtosphaera aculeata

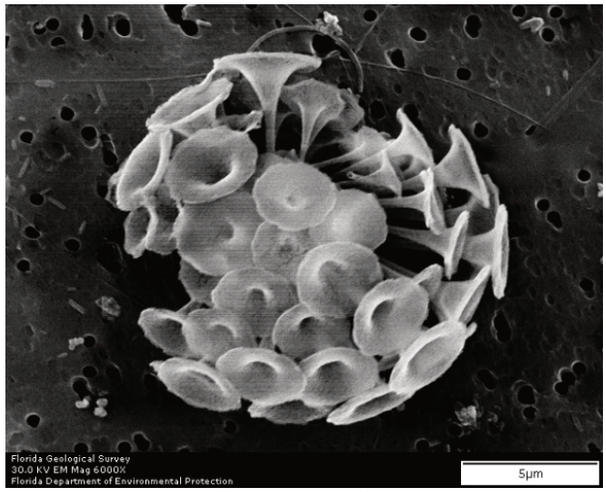

Discosphaera tubifera

Emiliania huxleyi

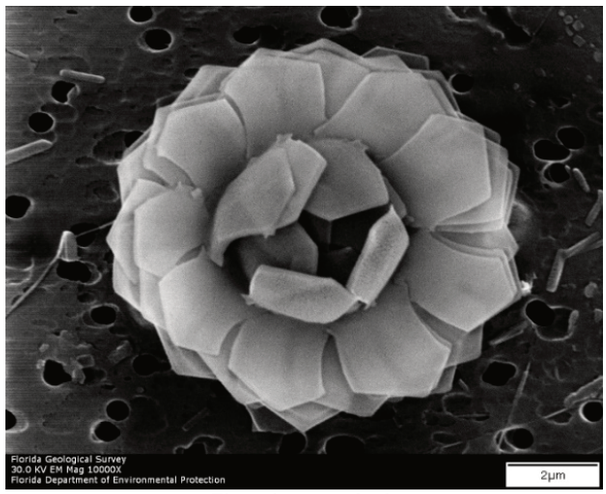

Florisphaera profunda

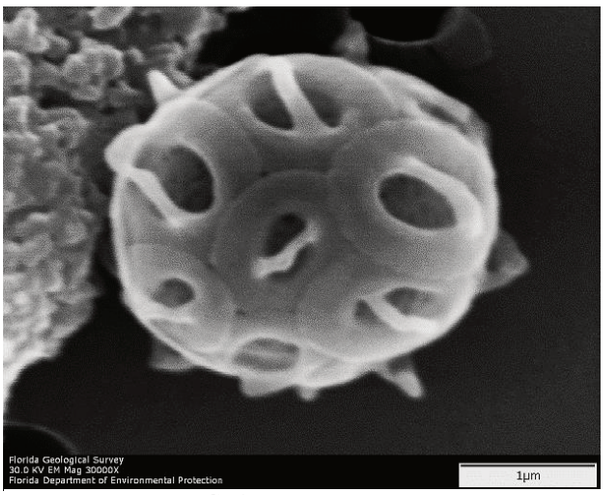

Gephyrocapsa ericsonii

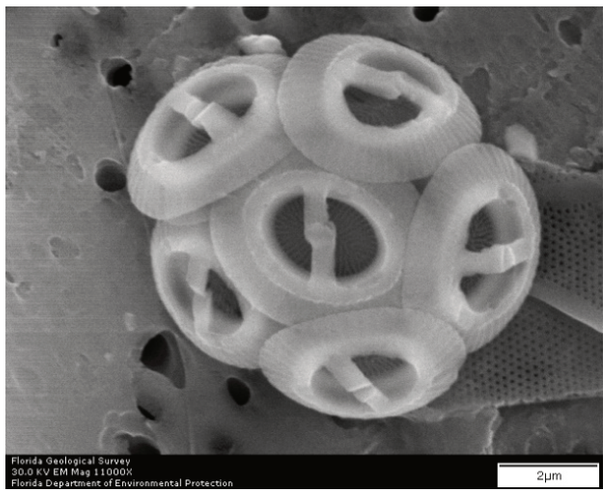

Gephyrocapsa oceanica

Plate 4

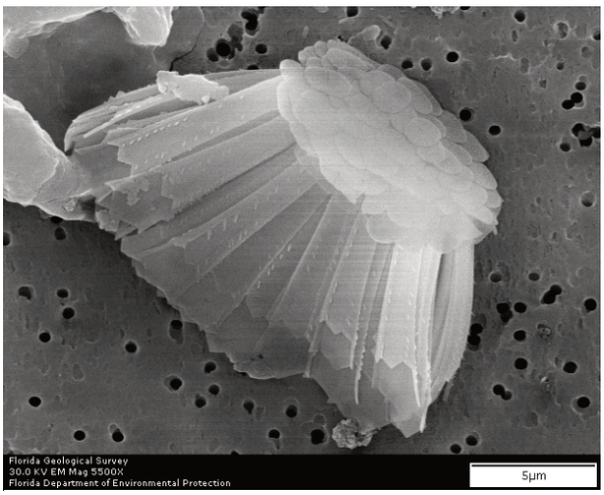

Gladiolithus flabellatus

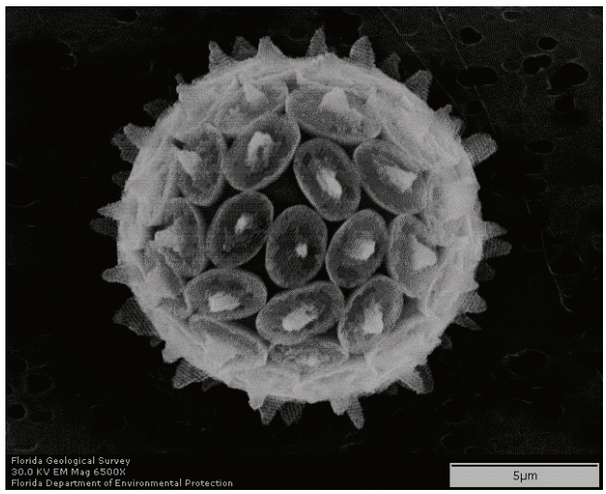

Helicosphaera HOL *catilliferus* type

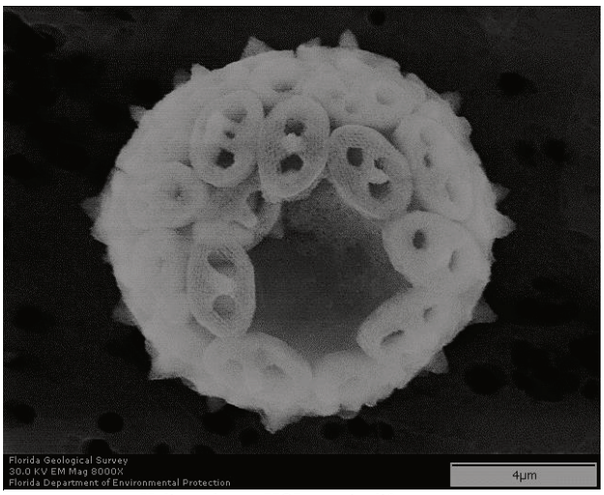

Helicosphaera HOL *ponticuliferus* type

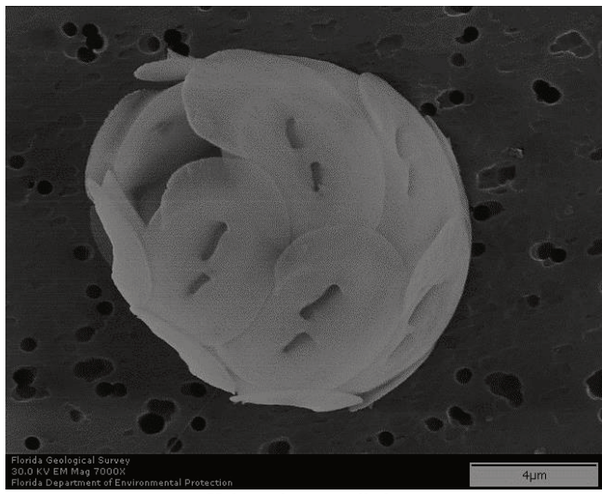

Helicosphaera wallichii

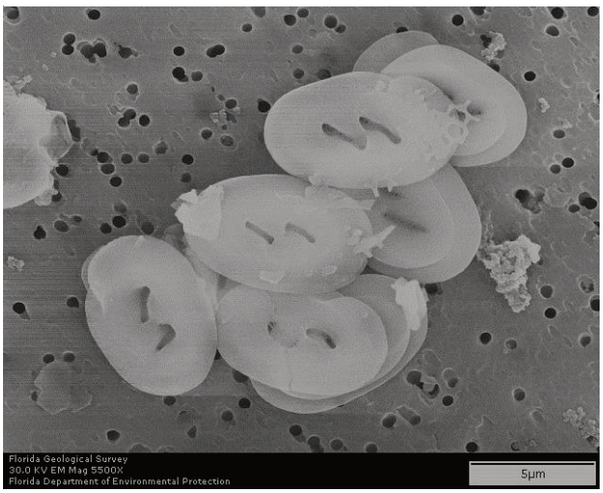

Helicosphaera wallichii coccoliths

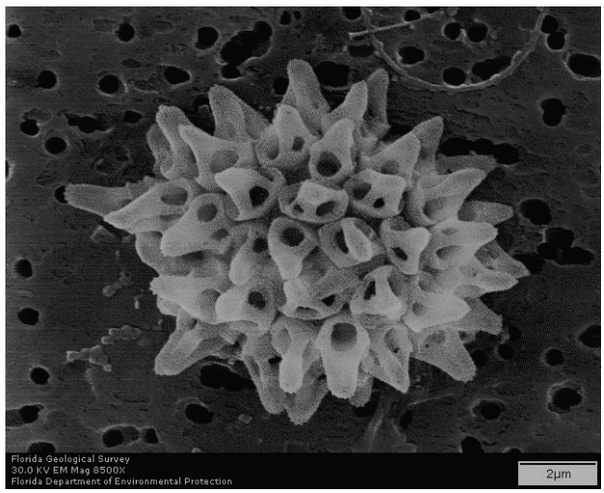

Homozygosphaera triarcha

Plate 5

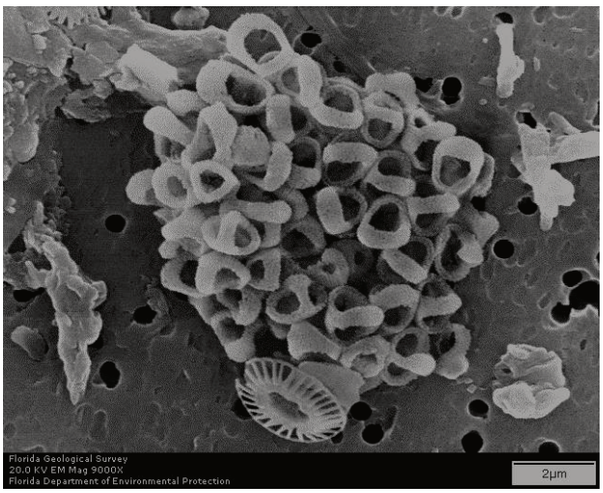

Homozygosphaera arethusae

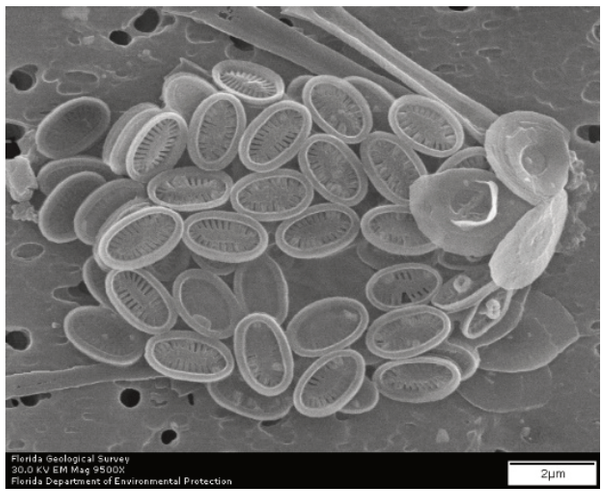

Michaelsarsia adriaticus

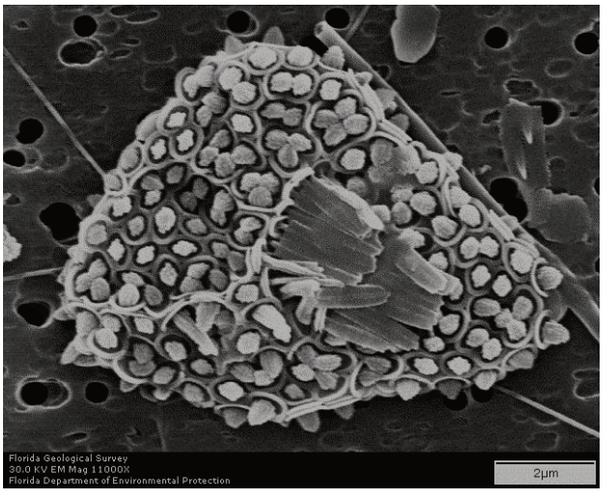

Navilithus altivelum

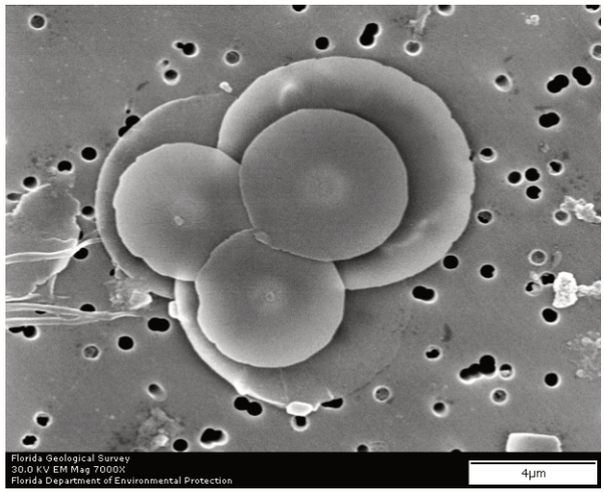

Oolithotus fragilis

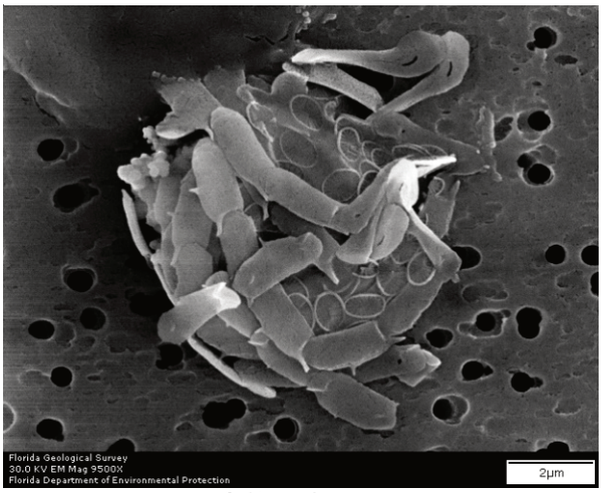

Ophiaster formosus

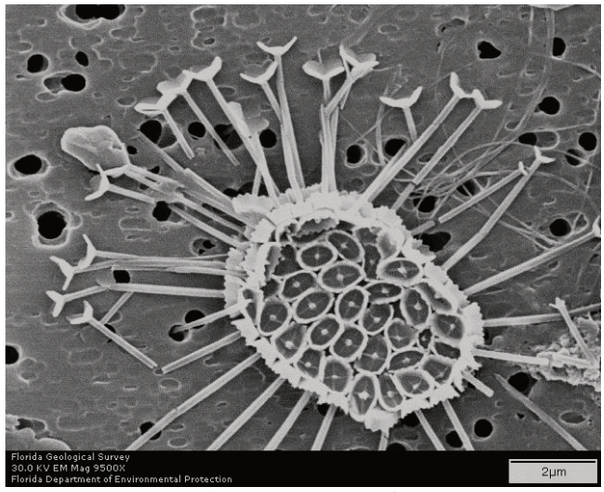

Pappamonas sp. type 3

Plate 6

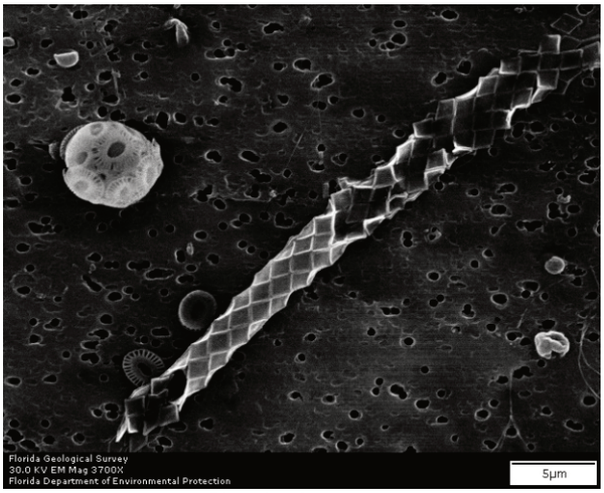

Placorhombus ziveriae

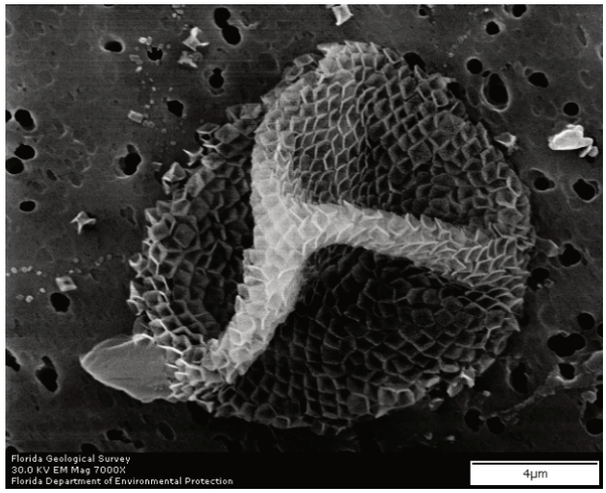

Polycrater galapagensis

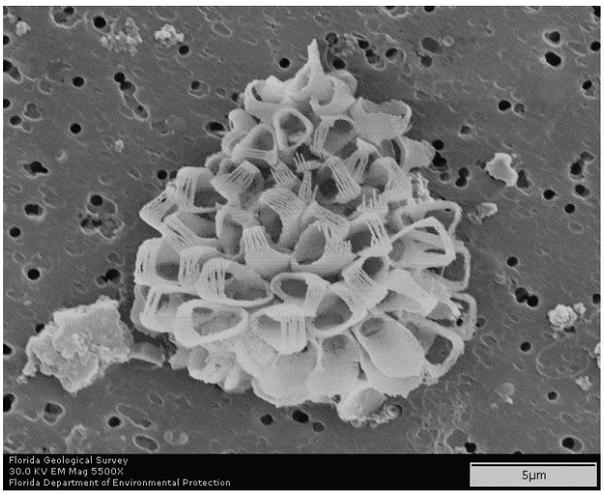

Poritectolithus maximus

Solisphaera galbula

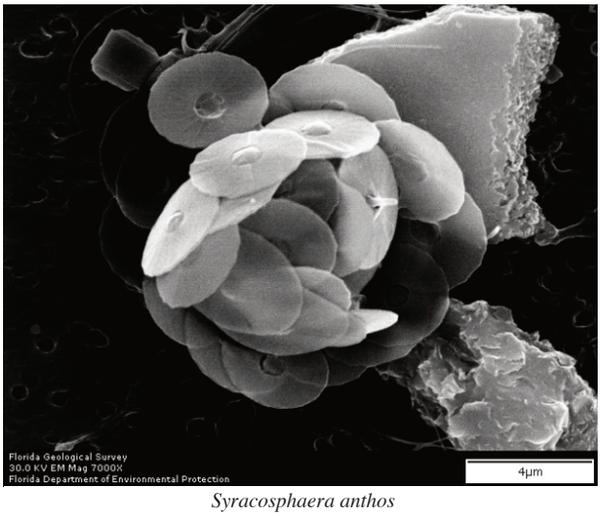

Syracosphaera anthos

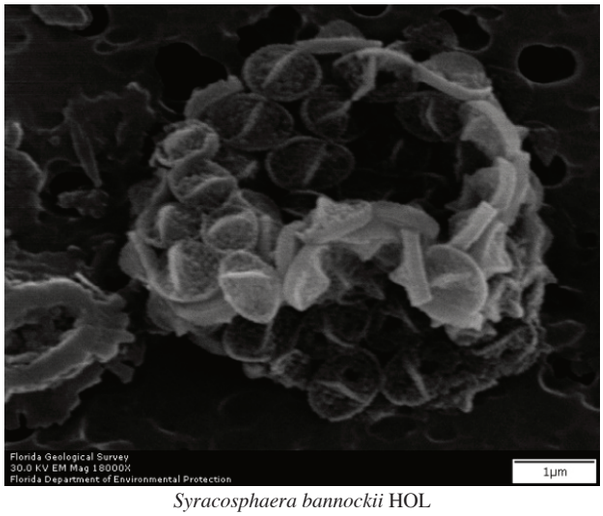

Syracosphaera bannockii HOL

Plate 7

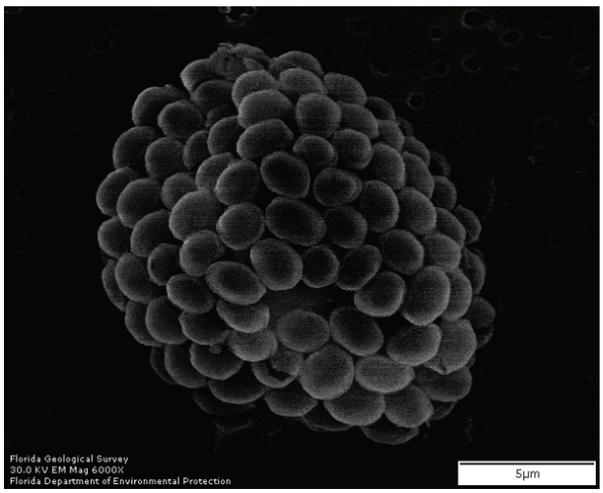

Syracosphaera pulchra HOL *oblonga* type

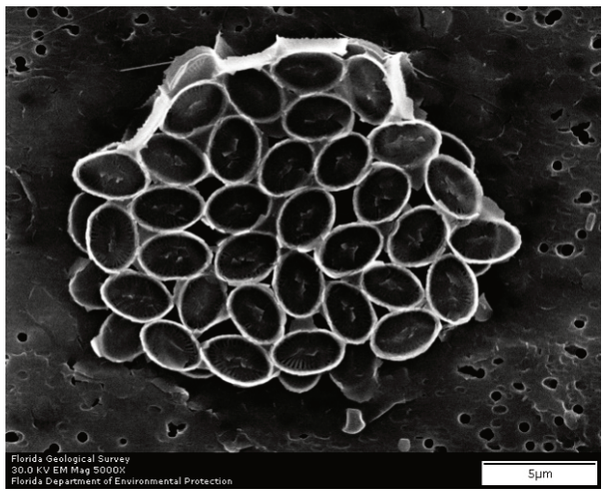

Syracosphaera tumularis

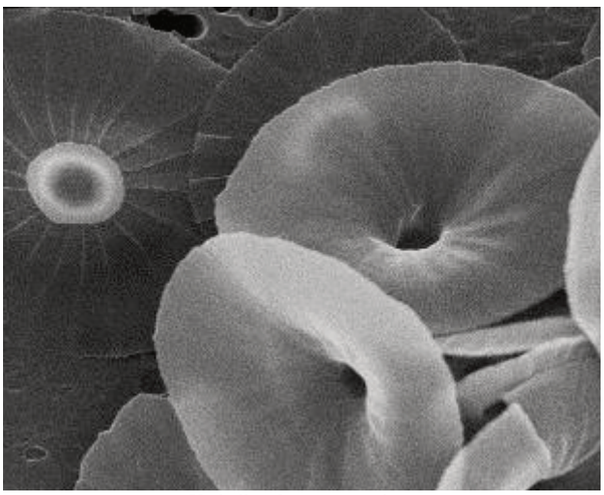

Umbellosphaera irregularis

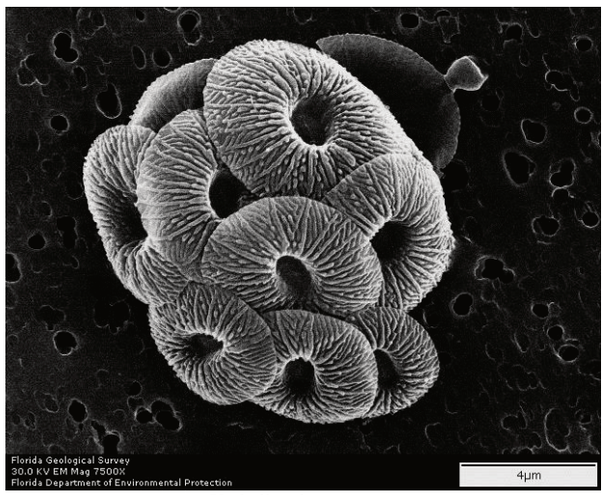

Umbellosphaera tenuis

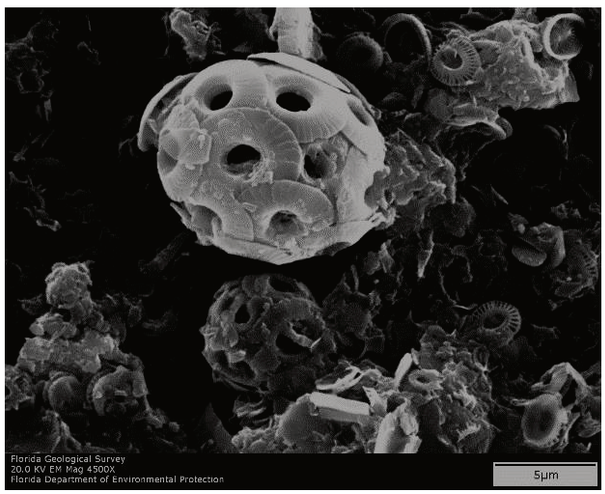

Umbilicosphaera foliosa

study was not long enough to thoroughly investigate such large-scale topics, but did provide the basis for continuing such an investigation.

A future phase of this project will involve a comparison of all the months in the three-year time period in order to investigate seasonal shifts in the species assemblages and the related ecological parameters. This could be performed for the sampling interval of 2011 to 2013 alone, but it would be preferable to continue sampling to perform a longer census. A 5- to 10-year sampling period would provide much better insights into the coccolithophore dynamics in the Gulf of Mexico. Such an in-depth investigation would provide useful insights into seasonal variations in species dynamics, possible tolerance variations controlling ecological niche selection, and the recovery of such trophic systems, from the bottom up, after major events. In the long run, this could help in the better planning of recovery efforts, and in estimating the timing of system degradation for any major future anthropogenic and/or environmental events.

Acknowledgements

We would like to thank the Deep-C Consortium for funding the project and Florida State University for providing lab space and resources. We would also like to acknowledge the scientists who helped collect samples on the *RV Bellows*, especially Dr James A. Nienow, who led many of the expeditions. We are indebted to Dr Lluïsa Cros, Prof Ric Jordan and Dr Jamie Shamrock for reviews and comments.

References

Bown, P.R. & Young, J.R. 1998. Techniques. *In*: P.R. Bown (Ed.). *Calcareous Nannofossil Biostratigraphy*. Chapman and Hall/Kluwer Academic, London: 16–28.

Brand, L.E. 1994. Physiological ecology of marine coccolithophores. *In*: A. Winter & W.G. Siesser (Eds). *Coccolithophores*. Cambridge University Press, Cambridge: 39–49.

Cruz, J., Young, J.R. & Wise, S.W., Jr. 2014. First observation of *Navilithus altivelum* in the Gulf of Mexico. *Journal of Nannoplankton Research*, **34**: 27–30.

Pariente, V. 1997. *Coccolithophores of the Gulf of Mexico and their relationship to water column properties*. Unpublished dissertation, Texas A&M University: 149 pp.

Siesser, W.G. & Winter, A. 1994. Composition and morphology of coccolithophore skeletons. *In*: A. Winter & W.G. Siesser (Eds). *Coccolithophores*. Cambridge University Press, Cambridge: 49–62.

Young, J.R., Geisen, M., Cros, L., Kleijne, A., Sprengel, C., Probert, I. & Østergaard, J. 2003. A guide to extant coccolithophore taxonomy. *Journal of Nannoplankton Research, Special Issue*, **1**: 125 pp.

Appendix 1 (next page)

Location of sampling sites with dates and times of collection.

Event ID	Site	Site coordinates (Lat +°N, Long +°E)	Date	Time	Event
BE-1204CT1	P1	(30.25, -87.25)	29/09/2011	13:30:00	CTD
BE-1204CT4	P2	(30.1666, -87.25)	29/09/2011	14:54:00	CTD
BE-1204CT5	P3	(30.0833, -87.25)	29/09/2011	16:09:00	CTD
BE-1204CT8	P4	(30, -87.25)	29/09/2011	17:36:00	CTD
BE-1204CT9	P5	(29.9166, -87.25)	29/09/2011	18:48:00	CTD
BE-1204CT12	P6	(29.8333, -87.25)	29/09/2011	20:15:00	CTD
BE-1204CT13	P7	(29.75, -87.25)	29/09/2011	21:59:00	CTD
BE-1204CT16	P8	(29.5833, -87.25)	30/09/2011	00:46:00	CTD
BE-1204CT17	P9	(29.4166, -87.25)	30/09/2011	03:18:00	CTD
BE-1204CT20	C9	(29.5, -86.6666)	30/09/2011	11:25:00	CTD
BE-1204CT23	C8	(29.6666, -86.6666)	30/09/2011	13:29:00	CTD
BE-1204CT24	C7	(29.8333, -86.6666)	30/09/2011	15:30:00	CTD
BE-1204CT27	C6	(29.9166, -86.6666)	30/09/2011	17:13:00	CTD
BE-1204CT28	C5	(30, -86.6666)	30/09/2011	18:58:00	CTD
BE-1204CT31	C4	(30.0833, -86.6666)	30/09/2011	20:38:00	CTD
BE-1204CT32	C3	(30.1666, -86.6666)	30/09/2011	22:01:00	CTD
BE-1204CT35	C2	(30.25, -86.6666)	30/09/2011	23:18:00	CTD
BE-1204CT36	C1	(30.3333, -86.6666)	01/10/2011	00:33:00	CTD
BE-1205CT1	A9	(29.5791, -86.1583)	24/10/2011	11:39:00	CTD
BE-1205CT4	A8	(29.6458, -86.1083)	24/10/2011	13:47:00	CTD
BE-1205CT5	A7	(29.7125, -86.0583)	24/10/2011	14:55:00	CTD
BE-1205CT8	A6	(29.7833, -86.0166)	24/10/2011	16:17:00	CTD
BE-1205CT9	A5	(29.8541, -85.9666)	24/10/2011	17:10:00	CTD
BE-1205CT12	A4	(29.9166, -85.9208)	24/10/2011	18:30:00	CTD
BE-1205CT13	A3	(29.9916, -85.8666)	24/10/2011	19:27:00	CTD
BE-1205CT16	A2	(30.0666, -85.8166)	25/10/2011	03:46:00	CTD
BE-1205CT17	A1	(30.1333, -85.775)	24/10/2011	21:35:00	CTD
BE-1205CT20	C1	(30.3333, -86.6666)	25/10/2011	11:54:00	CTD
BE-1205CT23	C2	(30.25, -86.6666)	25/10/2011	12:56:00	CTD
BE-1205CT24	C3	(30.1666, -86.6666)	25/10/2011	13:52:00	CTD
BE-1205CT27	C4	(30.0833, -86.6666)	25/10/2011	14:59:00	CTD
BE-1205CT28	C5	(30, -86.6666)	25/10/2011	16:15:00	CTD
BE-1205CT31	C6	(29.9166, -86.6666)	25/10/2011	18:00:00	CTD
BE-1205CT32	C7	(29.8333, -86.6666)	25/10/2011	19:30:00	CTD
BE-1205CT35	C8	(29.6666, -86.6666)	25/10/2011	22:08:00	CTD
BE-1205CT36	C9	(29.5, -86.6666)	26/10/2011	00:17:00	CTD
BE-1205CT39	D1	(29.293, -87)	26/10/2011	04:34:00	CTD
BE-1205CT42	P9	(29.4166, -87.25)	26/10/2011	11:45:00	CTD
BE-1205CT45	P8	(29.5833, -87.25)	26/10/2011	14:32:00	CTD
BE-1205CT46	P7	(29.75, -87.25)	26/10/2011	16:39:00	CTD
BE-1205CT49	P6	(29.8333, -87.25)	26/10/2011	18:14:00	CTD
BE-1205CT50	P5	(29.9166, -87.25)	26/10/2011	19:25:00	CTD
BE-1205CT53	P4	(30, -87.25)	26/10/2011	20:34:00	CTD
BE-1205CT54	P3	(30.0833, -87.25)	26/10/2011	21:33:00	CTD
BE-1205CT57	P2	(30.1666, -87.25)	26/10/2011	22:36:00	CTD
BE-1205CT58	P1	(30.25, -87.25)	26/10/2011	23:33:00	CTD
BE-1307CT1	P1	(30.25, -87.25)	13/10/2012	07:58:07	CTD
BE-1307CT4	P3	(30.0833, -87.25)	13/10/2012	10:01:10	CTD
BE-1307CT7	P5	(29.9166, -87.25)	13/10/2012	12:04:13	CTD

Event ID	Site	Site coordinates (Lat +°N, Long +°E)	Date	Time	Event
BE-1307CT10	C7	(29.8333, -86.6666)	13/10/2012	16:43:04	CTD
BE-1307CT13	C5	(30, -86.6666)	13/10/2012	18:46:07	CTD
BE-1307CT16	C3	(30.1666, -86.6666)	13/10/2012	20:49:10	CTD
BE-1307CT19	C1	(30.3333, -86.6666)	13/10/2012	22:52:13	CTD
BE-1307CT22	D1	(29.293, -87)	14/10/2012	07:46:27	CTD
BE-1307CT25	D1	(29.293, -87)	14/10/2012	07:46:27	CTD
BE-1307CT26	P7	(29.75, -87.25)	14/10/2012	13:04:21	CTD
BE-1307CT29	P7	(29.75, -87.25)	14/10/2012	13:04:21	CTD
BE-1403CT3	P1	(30.25, -87.25)	14/09/2013	10:45:00	CTD
BE-1403CT4	P2	(30.1666, -87.25)	14/09/2013	11:20:00	CTD
BE-1403CT7	P3	(30.0833, -87.25)	14/09/2013	12:26:00	CTD
BE-1403CT8	P4	(30, -87.25)	14/09/2013	13:50:00	CTD
BE-1403CT11	P5	(29.9166, -87.25)	14/09/2013	15:15:00	CTD
BE-1403CT12	P6	(29.8333, -87.25)	14/06/2013	16:30:00	CTD
BE-1403CT14	P7	(29.75, -87.25)	14/09/2013	17:21:00	CTD
BE-1403CT16	P8	(29.5833, -87.25)	14/09/2013	19:43:00	CTD
BE-1403CT19	P9	(29.4166, -87.25)	14/09/2013	21:26:00	CTD
BE-1403CT22	A9	(29.5791, -86.1583)	15/09/2013	06:38:00	CTD
BE-1403CT23	A8	(29.6458, -86.1083)	15/09/2013	08:03:00	CTD
BE-1403CT26	A7	(29.7125, -86.0583)	15/09/2013	08:48:00	CTD
BE-1403CT27	A6	(29.7833, -86.0166)	15/09/2013	09:54:00	CTD
BE-1403CT30	A5	(29.8541, -85.9666)	15/09/2013	10:46:00	CTD
BE-1403CT31	A4	(29.9166, -85.9208)	15/09/2013	11:58:00	CTD
BE-1403CT34	A3	(29.9916, -85.8666)	15/09/2013	13:00:00	CTD
BE-1403CT35	A2	(30.0666, -85.8166)	15/09/2013	13:56:00	CTD
BE-1403CT38	A1	(30.1333, -85.775)	15/09/2013	14:36:00	CTD
BE-1403CT41	C9	(29.5, -86.6666)	15/09/2013	23:30:00	CTD
BE-1403CT42	C8	(29.6666, -86.6666)	16/09/2013	02:24:00	CTD
BE-1403CT45	C7	(29.8333, -86.6666)	16/09/2013	04:04:04	CTD
BE-1403CT46	C6	(29.9166, -86.6666)	16/09/2013	04:15:00	CTD
BE-1403CT49	C5	(30, -86.6666)	16/09/2013	05:05:00	CTD
BE-1403CT50	C4	(30.0833, -86.6666)	16/09/2013	07:45:00	CTD
BE-1403CT53	C3	(30.1666, -86.6666)	16/09/2013	08:53:00	CTD
BE-1403CT54	C2	(30.25, -86.6666)	16/09/2013	09:56:00	CTD
BE-1403CT55	C1	(30.3333, -86.6666)	16/09/2013	10:45:00	CTD

Appendix 2

Alphabetical list of all taxa encountered in this study.

Acanthoica quattrospina Lohmann, 1903 (holococcolith in Cros et al., 2000)

Algirosphaera robusta (Lohmann, 1902) Norris, 1984

Alisphaera gaudii Kleijne et al., 2002

A. ordinata (Kamptner, 1941) Heimdal, 1973

A. pinnigera Kleijne et al., 2002

Alveosphaera bimurata (Okada & McIntyre, 1977) Jordan & Young, 1990

Calcidiscus leptoporus (Murray & Blackman, 1898) Loeblich & Tappan, 1978

Calciopappus caudatus Gaarder & Ramsfjell, 1954

C. rigidus Heimdal *in* Heimdal & Gaarder, 1981

Calciosolenia murrayi Gran, 1912

Calicasphaera diconstricta Kleijne, 1991

Calyptrolithina divergens (Halldal & Markali, 1955) Heimdal, 1982

C. multipora (Gaarder *in* Heimdal & Gaarder, 1980) Norris, 1985

Calyptrolithophora papillifera (Halldal, 1953) Heimdal *in* Heimdal & Gaarder, 1980

Ceratolithus cristatus Kamptner, 1950

C. cristatus HET *coccolithomorpha* type (Lecal-Schlauder, 1950) Young et al., 2003

Coccolithus pelagicus (Wallich, 1877) Schiller, 1930

Corisphaera strigilis Gaarder, 1962

Coronosphaera mediterranea (Lohmann, 1902) Gaarder *in* Gaarder & Heimdal, 1977

Cyrtosphaera aculeata (Kamptner, 1941) Kleijne, 1992

Discosphaera tubifera (Murray & Blackman, 1898) Ostenfeld, 1900

Emiliania huxleyi (Lohmann, 1902) Hay & Mohler *in* Hay et al., 1967

Florisphaera profunda Okada & Honjo, 1973

Gephyrocapsa ericsonii McIntyre & Bé, 1967

G. mullerae Bréhéret, 1978

G. oceanica Kamptner, 1943

Gladiolithus flabellatus (Halldal & Markali, 1955) Jordan & Chamberlain, 1993

Helicosphaera carteri (Wallich, 1877) Kamptner, 1954

H. HOL *ponticuliferus* type Young, 2014

H. wallichii (Lohmann, 1902) Okada & McIntyre, 1977

Helladosphaera cornifera (Schiller, 1913) Kamptner, 1937

Homozygosphaera arethusae (Kamptner, 1941) Kleijne, 1991

H. spinosa (Kamptner, 1941) Deflandre, 1952

H. triarcha Halldal & Markali, 1955

Hyalolithus neolepis Yoshida et al., 2006

Michaelsarsia adriaticus (Schiller, 1914) Manton et al., 1984

M. elegans Gran, 1912

Navilithus altivelum Young & Andruleit, 2006

Oolithotus fragilis (Lohmann, 1912) Martini & Müller, 1972

Ophiaster formosus Gran, 1912

Pappomonas sp.

Papposphaera sp.

Placorhombus ziveriae Young & Geisen *in* Young et al., 2003

Polycrater galapagensis Manton & Oates, 1980

Poritectolithus maximus Kleijne, 1991

Reticulofenestra sessilis (Lohmann, 1912) Jordan & Young, 1990

Scyphosphaera apsteinii Lohmann, 1902

Solisphaera spp.

S. galbula Kahn & Aubry *in* Aubry & Kahn, 2007

Syracolithus spp.

Syracosphaera anthos (Lohmann, 1912) Janin, 1987

S. bannockii HOL (Borsetti & Cati, 1976) Cros et al., 2000

S. pulchra HOL *oblonga* type Young et al., 2003

Syracosphaera spp.

S. tumularis Sánchez-Suárez, 1990

Thoracosphaera spp.

Umbilicosphaera anulus Young et al., 2003

U. foliosa (Kamptner, 1963) Geisen *in* Sáez et al., 2003

U. sibogae (Weber-van Bosse, 1901) Gaarder, 1970

Umbellosphaera irregularis Paasche *in* Markali & Paasche, 1955

U. tenuis (Kamptner, 1937) Paasche *in* Markali & Paasche, 1955